2010

Autonomous operation of wind-battery hybrid power system with maximum power extraction capability

Nishad Mendis
University of Wollongong, nnrm786@uowmail.edu.au

Kashem Muttaqi
University of Wollongong, kashem@uow.edu.au

Saad Sayeef
University of Wollongong, saad@uow.edu.au

Sarath Perera
University of Wollongong, sarath@uow.edu.au

Autonomous operation of wind-battery hybrid power system with maximum power extraction capability

Abstract

The hybrid operation of a remote area power system consisting of a Doubly Fed Induction Generator (DFIG) based wind turbine, a battery storage unit and a dummy load is investigated in this paper. The battery storage unit operates as a source or load, depending on the wind power output and loading conditions of the system. The battery storage is connected to the AC side of the wind energy system through a three phase inverter to supply both active and reactive power. A dummy load is also incorporated into the AC side of the system. The design criteria of the controllers for each component (ie. DFIG, battery storage system and dummy load) and an approach for control coordination of the entire system are presented in this paper. The suitability of the proposed control coordination strategy and individual system controllers are tested in relation to the system voltage, frequency and DC link stability of the DFIG under variable wind and changing load conditions. The maximum power extraction capability from wind is also achieved throughout the operation.

Disciplines

Physical Sciences and Mathematics

Publication Details

N. Mendis, K. M. Muttaqi, S. Sayeef & S. Perera, "Autonomous operation of wind-battery hybrid power system with maximum power extraction capability," in 2010 International Conference on Power System Technology (POWERCON), 2010, pp. 1-7.

2010 International Conference on Power System Technology

Autonomous Operation of Wind-Battery Hybrid Power System with Maximum Power Extraction Capability

Nishad Mendis, *Student Member, IEEE,*, Kashem M. Muttaqi, *Senior Member, IEEE*, Saad Sayeef, *Member, IEEE,* and Sarath Perera, *Member, IEEE*

***Abstract*—The hybrid operation of a remote area power system consisting of a Doubly Fed Induction Generator (DFIG) based wind turbine, a battery storage unit and a dummy load is investigated in this paper. The battery storage unit operates as a source or load, depending on the wind power output and loading conditions of the system. The battery storage is connected to the AC side of the wind energy system through a three phase inverter to supply both active and reactive power. A dummy load is also incorporated into the AC side of the system. The design criteria of the controllers for each component (ie. DFIG, battery storage system and dummy load) and an approach for control coordination of the entire system are presented in this paper. The suitability of the proposed control coordination strategy and individual system controllers are tested in relation to the system voltage, frequency and DC link stability of the DFIG under variable wind and changing load conditions. The maximum power extraction capability from wind is also achieved throughout the operation.**

***Index Terms*—Doubly fed induction generator, Battery storage system, Dummy load and Maximum power extraction.**

I. Introduction

ENERGY demand in most rural and regional communities in developed and developing countries are steadily increasing. Usually, such communities are located far away from the main grid. Supplying electricity to such places, through existing grids may not be possible due to the high cost associated with grid expansion [1] - [2]. Most of these isolated places are supplied using diesel generator systems because of their low installation cost, reliability and simplicity of operation. However, the fuel cost and environmental concerns make this option less favourable. Instead, hybrid Remote Area Power Supply Systems (RAPS) are now being considered as a new emerging technology in supplying electricity to isolated or remote areas including islands [3]. Usually, hybrid power systems have more than one energy source and may consist of different renewable energy sources such as wind, solar, micro hydro, etc. However, the selection of a suitable generation mix is entirely site specific depending on the availability of the renewable energy sources. Design and operation of RAPS is quite a challenging task as the system operation is totally independent from the main grid supply. Also, RAPS systems can be characterised with lower X/R ratio, lower system inertia and coupling effect between active and reactive power. With these challenges, the voltage and frequency of the system have to be maintained within acceptable limits as they are the most important parameters to be controlled in the customer perspective. In addition, coordinated control, optimised operation and power quality control of the system are the other key aspects of hybrid RAPS systems [4]- [5].

Wind is identified as one of the fastest growing renewable energy technologies in the energy industry. However, the operation of wind generator based power systems are challenging due to the variable and intermittent nature of wind. When a wind generator is operated in grid connected mode, power smoothing/conditiong and other power quality aspects (ie. harmonics and flicker) are the most important aspects to be examined whereas in the standalone mode, the highest emphasis is given to minimise the demand-generation mismatch to overcome unexpected voltage and frequency excursions [6]. An Energy Storage System (ESS) is an attractive and promising solution to manage such issues. Widely used or advocated energy storage technologies for wind farms are batteries, super capacitors, flywheel energy storage systems and Super Conducting Magnetic Energy Storage (SMES) systems [7]. For a standalone wind generator based power system, a battery storage system is seen to be the best option as it contains high energy density compared to other available energy storage systems (ie. super capacitors, SMES). Among various wind turbine generator technologies available, Doubly Fed Induction Generator (DFIG) is recommended for high power applications [8]. It offers many advantages over other types of wind turbine generators which can be found in [9]. In standalone power systems, it is a common practice to incorporate a dummy load into the system to absorb any additional power associated with over generation which cannot be handled by an energy storage system.

Relevant research work include the application of an ESS for grid connected wind applications with DC/DC converter interface [10] - [11]. The operation of a hybrid power system consisting of an induction generator based wind turbine system, an inverter assisted battery storage unit and a dummy load is discussed in [12]. However, the standalone operation of a DFIG based RAPS system has not received much research attention when compared to its grid connected operation. Also, the Maximum Power Extraction (MPE) capability from wind is important if a variable speed wind generator is

Mr. Nishad Mendis, A/Prof. Kashem M. Muttaqi, Dr. Saad Sayeef and A/Prof. Sarath perera are with the School of Electrical, Computer and Telecommunications Engineering, University of Wollongong, and are Members of the Integral Energy Power Quality and Reliability Centre, NSW 2522, Australia (email: nnrm786@uow.edu.au).

978-1-4244-5940-7/10/$26.00©2010 IEEE

used for power generation to ensure optimised operation. The maximum power extraction from wind using a DFIG in grid connected environments is explained in [13] - [14]. However, the MPE capability of the DFIG using an ESS for its standalone operation is not thoroughly investigated in the existing literature.

A novel hybrid RAPS system considered in this paper, consisting of a DFIG, dummy load and its controller, battery storage system as the preferred ESS and main loads, is shown in Fig. 1. The reactive power demand of the system is provided through the DFIG and battery inverter. In this regard, the DFIG is considered as the main source which has to provide the highest portion of the reactive power requirement of the system. Also, the battery inverter system is designed to provide a fixed quantity of reactive power to the system when necessary. In addition, the active power requirement of the system is achieved through a control coordination strategy which facilitates to minimise the active power imbalance of the system while extracting maximum power from wind.

The paper is organised as follows. Section II outlines the concept of maximum power point tracking from wind. The control methodologies of the DFIG based remote area power system covering Rotor Side Converter (RSC) and Line Side Converter (LSC) are given in Section III. Section IV discusses the adopted control coordination methodology for the RAPS system. Individual control strategies adopted for the battery and dummy load are discussed in Section V. Section VI examines the simulated behaviour of the RAPS system under variable wind and changing load conditions. Conclusions are given in Section VII.

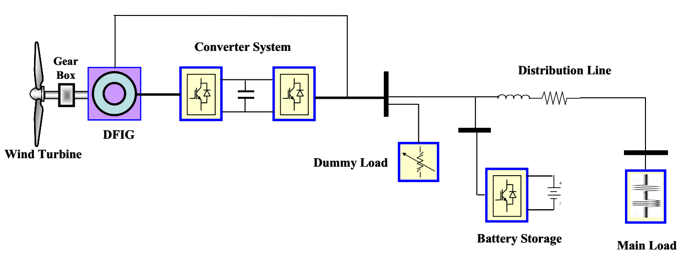

Fig. 1. Proposed hybrid RAPS system

II. Maximum Power Extraction from Wind

The power captured from the wind turbine is given by (1). However, the power coefficient, C_p, of the wind turbine is a function of tip speed ratio, λ, and pitch angle, β. The maximum power from wind can be obtained when the wind turbine operates at its optimum power coefficient $(C_\mathrm{p})_\mathrm{opt}$. This can be achieved by operating the turbine at a desired speed to obtain the optimised tip speed ratio given by (2). The MPE from wind, without considering the associated system losses (ie. ideal condition), can be described using (7) as given in [13] - [14]. The power losses associated with inverters have also been considered when implementing the maximum power extraction algorithm, although it is not included in (1) - (7). The turbine power characteristics with MPE curve described by (7) is shown in Fig. 2.

$$P_m = \frac{1}{2}C_p(\lambda,\beta)A\rho v^3 \tag{1}$$

$$\lambda_{opt} = \frac{(\omega_r)_{opt}R}{v} \tag{2}$$

$$v = \frac{(\omega_r)_{opt}}{\lambda_{opt}} \tag{3}$$

$$P_m = \frac{1}{2}(C_p)_{opt}A\rho\frac{[(\omega_r)_{opt}]^3R^3}{\lambda_{opt}^3} \tag{4}$$

$$(P_m)_{opt} = \frac{1}{2}(C_p)_{opt}\rho A(\frac{R}{\lambda_{opt}})^3[\omega_{ropt}]^3 \tag{5}$$

$$k_{opt} = \frac{1}{2}(C_p)_{opt}\rho A(\frac{R}{\lambda_{opt}})^3 \tag{6}$$

$$(P_m)_{opt} = k_{opt}[(\omega_r)_{opt}]^3 \tag{7}$$

where,
P_m- power output from the turbine, C_p- power coefficient of wind turbine, A- cross sectional area of the wind turbine blade, v- wind speed, ρ- air density, R- radius of blade, λ- tip speed ratio and $(P_m)_{opt}$- maximum mechanical power output from the wind

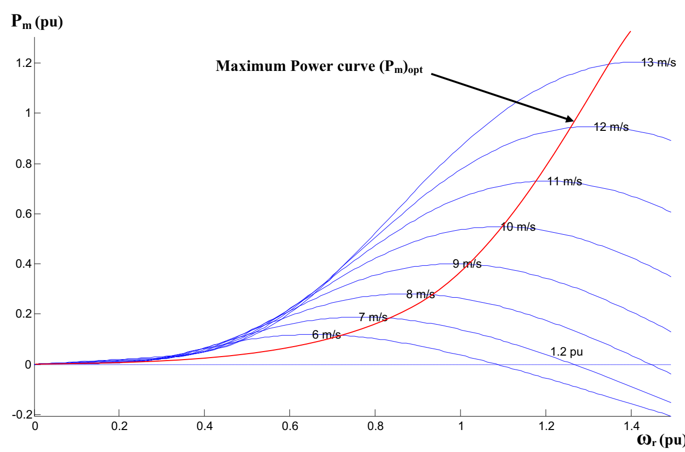

Fig. 2. Wind turbine power characteristics and maximum power extraction curve

III. Controls associated with DFIG

In the proposed hybrid RAPS system shown in Fig. 1, the DFIG acts as the main source of energy and thus has to contribute the most towards the control of system voltage and frequency. In this paper, vector control methodologies discussed in [15] have been taken as a basis to develop the control algorithms for the Rotor Side Converter (RSC) and Line Side Converter (LSC). Details of implementing the controls associated with the DFIG is not discussed in this paper as the hybrid operation of the entire system is the major subject of interest.

The rotor side converter is used to control the system AC voltage and frequency. The voltage control through the DFIG has been implemented using the reactive power control approach, which can be mathematically explained using (8) - (13). Also, it can be seen that the *d* component of rotor current, i_{rd}, is used to control the reactive power provision from the

DFIG. To achieve better voltage regulation, the total reactive power supplied by the DFIG is divided into two components (ie. Q_{gen} and Q_{mag}). The fraction given by Q_{gen} is used to provide the reactive power required by the system loads whereas, Q_{mag} represents the magnetising reactive power (ie. no load reactive power) needed by the DFIG. However, this magnetising component is compensated by imposing the condition given in (13).

The frequency control of the system through the DFIG is implemented by using the conditions given in (14) - (15). These are the necessary and sufficient conditions that ensure the stator flux oriented mode of operation of the RSC. By implementing this condition, the frequency regulation of the DFIG is made to be independent from the machine speed as well as the resistive loading condition of the system. The complete control block diagram of the RSC is shown in Fig. 3.

The conventional LSC arrangement has been used in this paper. In this regard, the DC link voltage of the back to back converter system should be controlled regardless of the direction of power flow [15]. In addition, it can be modified to provide some reactive power to the system as mentioned in [16]. However, in this study, the reactive power supplementation through the LSC is set to zero (ie. unity power factor operation).

$$Q_s = -\frac{3}{2}V_{sq}i_{sd} \tag{8}$$

$$Q_s = Q_{mag} + Q_{gen} \tag{9}$$

$$Q_{gen} = \frac{3}{2}V_s\frac{L_m}{L_s}i_{rd\ gen} \tag{10}$$

$$Q_{mag} = 0 \tag{11}$$

$$Q_{mag} = \frac{3}{2}[-\frac{V_s^2}{\omega L_s} + V_s\frac{L_m}{L_s}i_{ms}] = 0 \tag{12}$$

$$i_{ms} = \frac{V_S}{\omega L_m} \tag{13}$$

$$\phi_{sq} = 0 \tag{14}$$

$$i_{sq} = i_{rq}(\frac{-L_m}{L_s}) \tag{15}$$

where,
Q_s- stator reactive power, i_{ms}- stator magnetising current, v_{sq}- stator q-axis voltage, i_{sd}- stator d-axis current, v_{sd}- stator d-axis voltage, i_{rd}- rotor d-axis current, ϕ_{sq}- stator flux q-component, L_m- DFIG magnetising inductance, L_s- magnetising inductance + stator leakage inductance

IV. Control coordination of RAPS system

As mentioned earlier, the control coordination among the system components has been implemented with a view to minimise the instantaneous active and reactive power imbalance associated with the system. To achieve acceptable frequency and voltage regulation of a RAPS system, the conditions given by (16) - (18) have to be satisfied and maintained. The reactive power sharing of the system is made between the DFIG and battery inverter system. In this paper, the battery inverter system is controlled to inject a predetermined amount

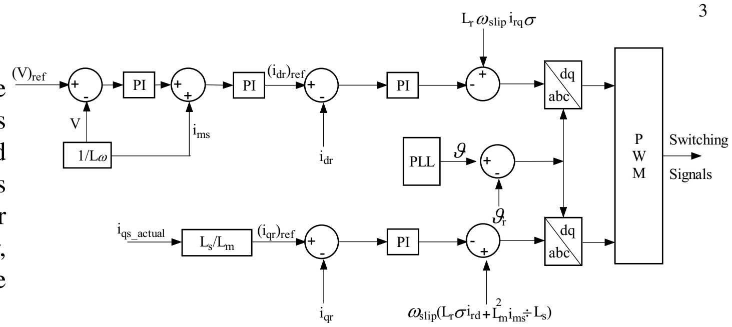

Fig. 3. Rotor side converter control

of reactive power into the system (ie. a fraction of minimum reactive power requirement of the RAPS system) while the remaining required reactive power is supplied by the DFIG as discussed in section III. With the control strategy suggested in Section III for DFIG, the frequency of the system is made independent from the loading condition and rotor speed of the DFIG. Hence, the system frequency cannot be used for control coordination purposes as suggested in [12]. Also, it is said that if a remote power system consists of only static loads, it is difficult to identify the frequency deviation of the system using active power imbalance and the voltage deviation from reactive power imbalance. Therefore, direct active power control has been used to develop the coordination strategy for the system in Fig. 1.

The active power sharing among the various system components is more crucial than the reactive power control in this RAPS system. Wind is identified as an uncontrolled energy source whereas the battery storage unit is identified as a controlled energy source. In this paper, the active power sharing among the system components is formulated taking two factors into consideration. The main objective is to minimise the generation-demand mismatch so as to avoid frequency and voltage excursions in the system. The other objective is to extract the maximum power from wind thus enabling the RAPS system to operate in its optimum mode of operation.

With the DFIG control strategies discussed in Section III, the RSC is fully configured to control the voltage and frequency of the system and hence MPE cannot be implemented within the inverter control as done in grid connected mode of operation. In this paper, a method to extract maximum wind power by using a battery storage unit and a dummy load is discussed. With the frequency control of the DFIG discussed in Section III, i_{sq} represents the active power of the load. Hence, any changes made to the main load is reflected as a change in i_{sq}, thereby i_{rq} and T_e as evident from (15) and (19) respectively. The MPE of the RAPS system is achieved by controlling the power flow of the battery storage system and dummy load. It is possible to impose an appropriate torque on the DFIG shaft to extract the maximum power from wind using the battery storage unit and dummy load. In this regard, the estimation of the reference battery power,$(P_b)_{ref}$, and reference dummy power, $(P_d)_{ref}$, have been estimated using the optimum wind power (ie. $(P_w)_{opt}$) taken as the reference wind power as expressed in (20) and (21) respectively.

The proposed control coordination strategy depicted in Fig.

4 is as follows. If the power output of the DFIG, P_w, is greater than the load power demand, P_L, the battery absorbs the additional power, $P_w - P_L$. Otherwise the battery storage will go into its discharge mode of operation. If the excess generation, P_w-P_L, is greater than the maximum rating of the battery, $(P_b)_{max}$, the dummy load has to consume the additional power associated with the RAPS system. If the dummy power, P_d, is higher than its maximum rating, $(P_d)_{max}$, then the wind turbine pitch regulation has to be activated to control the active power flow of the system. Further, it is assumed that P_w and P_b are sufficient to supply the system loads at all times.

$$\Sigma P_{sorces} - \Sigma P_{sinks} = \frac{dK.E}{dt} = \frac{d\Sigma(J\omega^2)}{dt} = 0 \quad (16)$$
$$P_w \pm P_b = P_L + P_d \quad (17)$$
$$\Sigma Q_{sources} - \Sigma Q_{sinks} = 0 \quad (18)$$

where,
P- active power, K.E- kinetic energy of the system, J- moment of inertia of rotating machine and ω- angular velocity of the rotating machine and Q- reactive power of the system

$$T_e = \frac{L_m}{L_s + L_m}\frac{V_s}{\omega_s} i_{rq} \quad (19)$$
$$(P_b)_{ref} = (P_w)_{opt} - P_L \quad (20)$$
$$(P_d)_{ref} = (P_w)_{opt} - P_L - (P_b)_{max} > 0 \quad (21)$$

where,
$(P_w)_{opt}$- MPE based wind power output (ie. electrical power) and T_e- electromagnetic torque of the DFIG

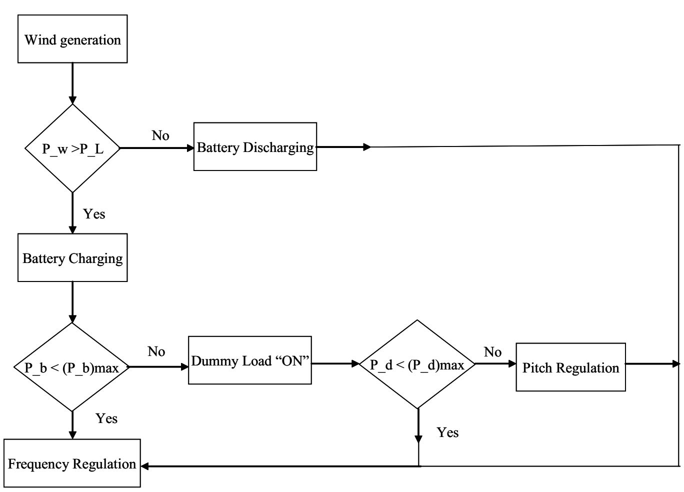

Fig. 4. Instantaneous power flow control of the proposed RAPS system

V. Supplementary Components control

The supplementary components of the proposed RAPS system in Fig. 1 are a dummy load and a battery storage system. When developing control strategies for the auxiliary components (ie. battery and dummy), the reference signals were derived using the instantaneous power imbalance of the system as described in section IV. The detailed information of individual control strategy associated with energy storage system and dummy load are discussed in the following subsections.

A. Energy Storage System

The battery storage in the RAPS system is used to minimise the generation-demand mismatch. In this paper, the operation of an inverter assisted battery storage unit is investigated. It is said that AC systems (eg. inverters) provide better and simpler control for energy exchange and has better performance compared to DC systems (eg. DC/DC converters). The synchronization of the battery inverter with the system is not discussed here as it is beyond the scope of this paper. The performance of the battery storage system is presented under variable wind and loading conditions.

The battery inverter system consists of IGBTs and is modelled as a Current Controlled Voltage Source Inverter. Fig. 5 shows the battery inverter model which was used to develop the associated vector control.

With the decoupled vector control, the active and reactive power of the inverter system can be given by (23) and (24) respectively. However, for the sake of simplicity, the reactive power supply through the inverter system is managed to provide a fixed amount of the system reactive power requirement. The estimation of the reference battery power (ie. $(P_b)_{ref}$ is discussed in Section IV. The active power of the battery system can be controlled using i_d as evident from (23). Therefore, the reference current of i_d is derived by comparing the reference power with the actual power drawn by the battery system (ie. P_b). The complete control diagram of the battery inverter control is shown in Fig. 6.

The estimation of the battery rating is a crucial subject as it depends on several factors such as site wind profile, total wind turbine inertia, low voltage ride through requirement, short circuit ratio, financial feasibility, etc. [6]. However, in this paper, the battery storage system capacity is estimated to supply a maximum of 0.35 pu power and the corresponding Ah rating can be estimated using (22). The standard battery model available in the MATLAB/Simpower System is used for the simulation purpose.

$$0.35 \times I_{rated} \times (\frac{t}{60}) = (Ah\ rating) \times k \quad (22)$$

where,
I_{rated}- rated capacity of the system, t- time duration that battery provides power into the system and k- average discharge/charge current of the battery in pu

$$P_b = v_d\, i_d \quad (23)$$
$$Q_b = v_d\, i_q \quad (24)$$

where,
P_b- active power output from the inverter, Q_b- reactive power output from the inverter, v_d- d component of the AC voltage of the inverter, i_d, i_q- d and q components of the inverter current

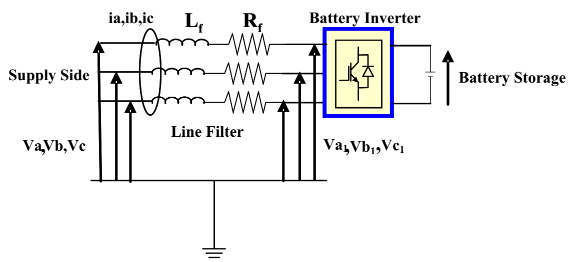

Fig. 5. Battery inverter model

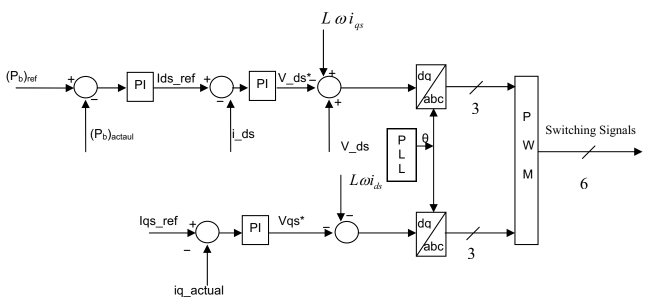

Fig. 6. Battery inverter controller

B. Dummy Load Controller

The dummy load is connected to the AC side of the system and consists of resistors. These resistors are connected across switches and the switching function is performed at zero crossing voltage to ensure minimum distortion level of the system voltage. The operation of the dummy load is enabled when it satisfies the condition given by (25). However, the dummy load has its own maximum capacity and is assumed to be 0.16 pu of the rated system capacity.

The estimation of dummy load reference power (ie. $(P_d)_{ref}$) is discussed in Section IV. This power signal is converted to a digital signal before sending it to the switches to perform the switching operation. The simplified control block diagram of the dummy load is shown in Fig. 7.

$$P_d \;=\; (P_w) + ((P_b)_{max} - P_L > 0 \tag{25}$$

where,
P_d- dummy load power and $(P)_{b\ max}$- maximum battery power

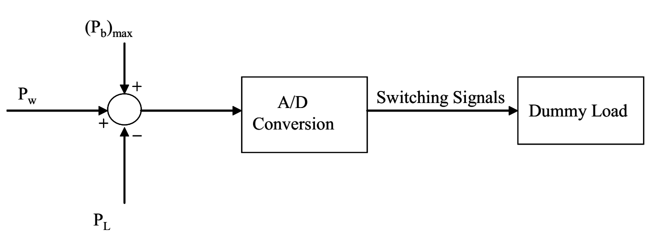

Fig. 7. Dummy load controller

VI. Simulation Results

The performance of the proposed wind/battery RAPS system has been evaluated under different system conditions. In this regard, changing wind profile, load (ie. resistive/inductive load) step up and an induction pump load connection to the system were considered. The robustness of the system is identified in relation to its voltage and frequency bandwidth regulation capability and stability of the DC link of the DFIG. The power sharing among system components together with MPE from the wind were also investigated.

The wind profile under which the system is simulated is shown in Fig. 8-(a). Initially, the wind speed is around 11 m/s and at t = 3.5 s, it drops to about to 9 m/s. The corresponding system voltage at the point of common coupling is shown in Fig. 8-(b). It can be seen that the system voltage stays within ± 0.02 pu under normal operation. At t = 2.5 s, a 0.04 pu rated induction pump load is connected to the system as seen in Fig. 9-(d). At the time of connection, the induction pump draws a relatively large amount of reactive current, which cannot be fully handled by the reactive power sources (ie. DFIG and battery inverter). Hence, the system voltage drops momentarily to a value of 0.9 pu. At t = 5 s, a load of 0.225 pu and power factor of 0.9 is introduced into the system. At this instance, due to the inability to supply the instant reactive power requirement, the voltage of the system drops again to a value of 0.96 pu. However, it recovers within 200 ms and returns to its rated value. The wind speed change that occurs at t = 3.5 s, is not seen to affect either the voltage or frequency. The frequency of the system is shown in Fig. 8-(c). It can be seen that the frequency of the system is regulated within ± 0.005 pu. The highest frequency deviation is seen to occur at t = 2.5 s (ie. at the time of induction pump load connection) due to the temporary loss of orientation of the system. As explained in Section III, the frequency control of the system through the DFIG is maintained by satisfying the conditions to ensure the adopted orientation schemes for both controllers (ie. RSC and LSC). However, at t = 2.5 s, the loss of orientation of the system contributes to a momentary frequency deviation in the system. This is due to the fact that the orientation schemes of the RSC and LSC are directly linked up with the system voltage. Again, the frequency of the system is not affected by the wind speed change, similar to the voltage response of the system. Also, as expected, the frequency of the system is not seen to be affected by the resistive load step up at t = 5 s. The DC link voltage of the back to back converter system of the DFIG is shown in Fig. 8-(d). The highest DC link voltage deviation is seen to occur at t = 2.5 s. The drop in the stator voltage is linked to the reduction in active power delivery to the load which causes the additional energy to return to the DC link resulting in a rise of DC link voltage to a high value as evident from Fig. 8-(d). According to the simulated behaviour, the DC link voltage variation is restricted within ± 0.03 pu.

The wind power variation of the system is shown in Fig. 9-(a). For simulation purposes, initially the slip of the wind turbine is set to s = -0.1 which corresponds to super synchronous mode of operation. From Fig. 9-(a), the wind power of the machine is seen to rise to a value of 0.625 pu. During this time, the load power consumption of the system is set to a value of 0.3 pu. The additional power is shared between the battery storage unit and dummy load as shown in Fig. 9-(b) and 9-(c) respectively. However, the maximum

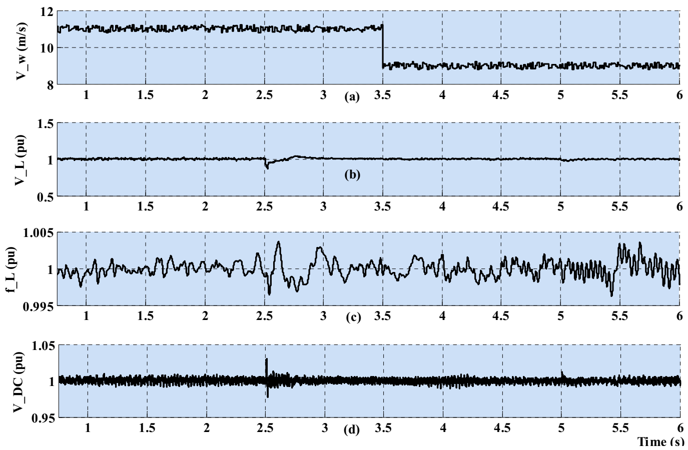

Fig. 8. Response of the RAPS system under variable wind and load conditions. (a) Wind velocity, (b) Load voltage, (c) Frequency and (d) DC link voltage

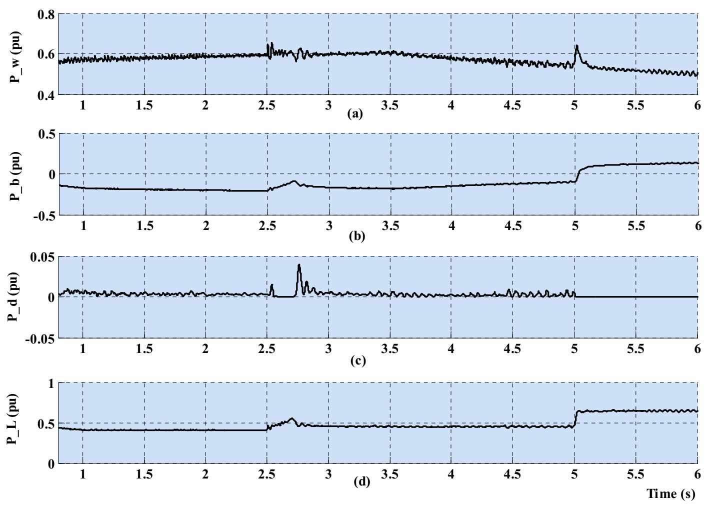

Fig. 9. Active power sharing of the RAPS system under variable wind and variable load conditions. (a) Wind power, (b) Battery power, (c) Dummy power and (d) Load demand

power capacity of the battery storage unit is limited to 0.35 pu. Hence, the remanning power (ie. $P_w - P_L - P_b$) is absorbed by the dummy load as evident from Fig. 9-(c). At time t = 3.5 s the wind velocity drops to 9 m/s causing a reduction in power output of the wind turbine generator. At the instance of resistive load step up, (ie. at t = 5 s), the load power exceeds the wind generator power output and the dummy load power is set to zero. At the same time, the battery changes its mode of operation from charging to discharging to maintain the system power balance.

Fig. 10 shows the actual wind power output (ie. P_w) and the optimal wind power (ie. $(P_w)_{opt}$). It can be seen that throughout the operation, the actual power output of the wind turbine generator follows the optimum power curve except during the load transients which are unavoidable.

VII. Conclusions

The hybrid operation of a DFIG, battery and dummy load is investigated under fluctuating wind and variable load conditions. The suitability of the proposed control coordination

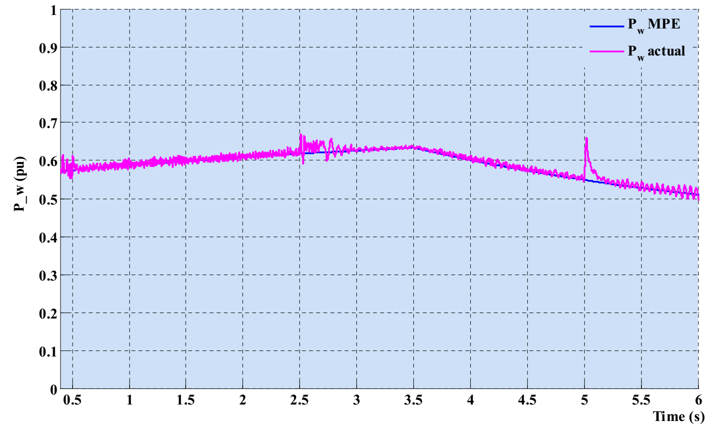

Fig. 10. Maximum power extraction from wind

strategy of the RAPS system is identified in terms of voltage and frequency regulation bandwidth, DC link stability of the DFIG and MPE capability. From the simulated behaviour, it is seen that the system voltage magnitude is regulated well except during the starting of the induction motor. The frequency of the system also stays within acceptable limits and not seen to be affected by the load step up as expected. The DC link voltage of the back-to-back converter system of the DFIG is maintained within acceptable limits except at the time of induction pump load connection. The maximum power extraction from the wind has been realised with the adopted control coordination for the RAPS system thus enabling optimised operation.

Acknowledgments

This work is supported by the Australian Research Council (ARC) and Hydro Tasmania Linkage Grant, LP0669245. The authors gratefully acknowledge the support and cooperation of Hydro Tasmania personnel in providing data and advice on the operation of remote area power supply system.

References

[1] T. Senjyu, T. Nakaji, K. Uezato and T. Funabashi, “A Hybrid Power System Using Alternative Energy Facilities in Isolated Island”, *IEEE Transaction on Energy Conversion*, vol. 20, issue 2, Jun 2005, pp. 406-414.

[2] V. V Rao and C. Chinnagounder, “Analysis of Hybrid Power Systems”, *First Asia International Conference on in Modelling and Simulation, Phuket, Thailand*, 27-30 Mar. 2007, pp. 1-8.

[3] Y. Hu and Z. Chen, “Modeling of Frequency and Power Control in An Autonomous Power System with Wind Turbines and Diesel Generation Units”, *Asia and Pacific, Transmission and Distribution Conference and Exhibition, Sydney, Australia*, 27-30 Mar. 2007, pp. 48-52.

[4] N. Mendis, K. Muttaqi and S. Perera, “Voltage quality behaviour of a wind turbine based Remote Area Power System”, *International Conference on Industrial Electronics, Gippsland, Australia* , 10-13 Feb. 2009, pp. 1-6.

[5] S. Sayeef, N. Mendis and K. Muttaqi, “Optimisation of Component Sizes for a Hybrid Remote Area Power Supply System”, *19th Australian Power Engineering Conference, Adelaide, Australia* , 27-30 Sept. 2009, pp. 1-6.

[6] C. A. Abbey and G. Joos, “Short-term energy storage for wind energy applications”, *Industry Application Conference, Hong Kong* , vol. 3, 2-6 Oct. 2005, pp. 2035-2042.

[7] L. Wei and G. Joos, “A Power Electronic Interface for a Battery Supercapacitor Hybrid Energy Storage System for Wind Applications”, *Power Electronics Specialists Conference, Rhodes, Greece* , 15-19 Jun. 2009.

[8] W. L. Kling and J. G. Slootweng, “Wind Turnines as Power Plants”, *IEEE/Cigre workshop on Wind Power and the Impacts on Power Systems, Oslo, Norway*, 17-18 Sept. 2002.

[9] S. Li and T.A Haskew,“Analysis of Decoupled d-q Vector Control in DFIG Back-to-Back PWM Converter”, *Power Engineering Society General Meeting, Tampa, Florida*, 24-28 Jun. 2007, pp. 1-7.

[10] J. Zhenhua and Y. Xunwei, “Modeling and control of an integrated wind power generation and energy storage system” *Power and Energy Society General Meeting, Calgary, Canada*, 26-30 Jul. 2009, pp. 1-8.

[11] A. Boyette, P. Poure and S. Sadate, “Constant Gird Power Control of Wind Turbines with DFIG and Long Duration Storage Unit” *International Journal of Distributed Energy Resources*, vol.3, Sept. 2006, pp. 63-82.

[12] R. Sebastian and J. Quesada, “Distributed Control System for frequency control in an islaoted wind system” *International Journal of Renewable energy - Science Direct*, vol.3, Mar. 2006, pp. 285-305.

[13] T. Luu and A. Nasiri, “Output power maximizing of a wind turbine by adjusting rotor speed” *Conference on Electrical and Computer Engineering, Ontario, Canada*, 4-7 May 2008, pp. 1591-1596.

[14] F. Yu, Q. L Liu and J. Zhang, “Flexible Grid-connection Technique and Novel Maximum Wind Power Tracking Algorithm for Doubly-Fed Wind Power Generator”, *IECON 33rd Annual Conference, Taipei, Taiwan*, 5-8 Nov. 2007, pp. 2098-2103.

[15] R. Pena, R. Cardenas, G. M. Asher J. C. Clare, J. Rodriguez and P. Cortes, “Vector Control of a Diesel-Driven Doubly Fed Induction Machine for a Stand-Alone Variable Speed Energy System”, *Industrial Electronics Society, 28th Annual Conference, Sevilla, Spain*, vol. 2, 5-8 Nov. 2002, pp. 985-990.

[16] M. Kayikci and J. V Milanovic, “Reactive Power Control Strategies for DFIG-Based Plants”, *IEEE Transaction on Energy Conversion*, vol. 22, issue 2, Jun. 2007, pp. 389-396.